

Assay Development for Histone Methyltransferases

Kurumi Y. Horiuchi, Mia M. Eason, Joseph J. Ferry,
Jamie L. Planck, Colin P. Walsh, Robert F. Smith,
Konrad T. Howitz, and Haiching Ma

Department of Biochemistry, Reaction Biology Corp., Malvern,
Pennsylvania.

ABSTRACT

Epigenetic modifications play a crucial role in human diseases. Unlike genetic mutations, however, they do not change the underlying DNA sequences. Epigenetic phenomena have gained increased attention in the field of cancer research, with many studies indicating that they are significantly involved in tumor establishment and progression. Histone methyltransferases (HMTs) are a large group of enzymes that specifically methylate protein lysine and arginine residues, especially in histones, using S-adenosyl-L-methionine (SAM) as the methyl donor. However, in general, HMTs have no widely accepted high-throughput screening (HTS) assay format, and reference inhibitors are not available for many of the enzymes. In this study, we describe the application of a miniaturized, radioisotope-based reaction system: the HotSpotSM platform for methyltransferases. Since this platform employs tritiated SAM as a cofactor, it can be applied to the assay of any HMT. The key advantage of this format is that any substrate can be used, including peptides, proteins, or even nucleosomes, without the need for labeling or any other modifications. Using this platform, we have determined substrate specificities, characterized enzyme kinetics, performed compound profiling for both lysine and arginine methyltransferases, and carried out HTS for a small-library LOPAC against DOT1L. After hit confirmation and profiling, we found that suramin inhibited DOT1L, NSD2, and PRMT4 with IC₅₀ values at a low μ M range.

INTRODUCTION

Epigenetics involves the study of changes in the regulation of gene activity and expression, independent of gene sequences. Post-translational modifications of histones, including methylation, acetylation, phosphorylation, and ubiquitination, are all important epigenetic factors. Histones are proteins around which DNA is wound for compaction and gene regulation. Two copies each of histones H2A, H2B, H3, and H4 assemble to form one nucleosome core, which is wrapped by ~146 base pairs of DNA. Histone H1 binds the nucleosome at the entry and

exit sites of the DNA and locks it into place.¹ The tight nucleosome structure helps to pack the entire genome into the cell nucleus and can restrict the access of nuclear factors to the DNA. This inherently restrictive environment must be tightly regulated to ensure that permissive cellular processes such as gene transcription, replication, recombination, and repair occur only under the appropriate circumstances. Because the dysfunction of these systems is inherent in many disease states, epigenetics has become an emerging frontier for drug discovery.

The human genome encodes more than 70 enzymes that catalyze the methylation of lysine (Lys, K) or arginine (Arg, R) residues on histones H1, H2A, H2B, H3, and H4. They are collectively referred to as histone methyltransferases (HMTs). HMTs mainly methylate histones using S-adenosyl-L-methionine (AdoMet or SAM) as a methyl donor.^{2,3} Most histone lysine methyltransferases (HKMTs) contain a SET-domain [Su(var)3-9, Enhancer of Zeste, and Trithorax]. The only known HKMTs that lack the SET domain are the members of the DOT1 family.⁴

Irregular expression of HKMTs is associated with human cancers.^{5,6} Enhancer of zeste homolog 2 (EZH2) is ubiquitously expressed during early embryogenesis, and becomes restricted to the central and peripheral nervous systems and the sites of fetal hematopoiesis during later development.⁷ EZH2 is responsible for the methylation of Lys 27 of histone H3⁸ as well as that of Lys 26 on histone H1.⁹ Overexpression of EZH2 is found in many cancers: prostate (metastatic), breast, liver, bladder, colon, skin, and lung, among others. However, surprising findings by Ernst and colleagues¹⁰ have suggested that EZH2 is a tumor suppressor in myeloid malignancies. G9a and G9a-like protein (GLP), the two highly homologous HKMTs, methylate Lys 9 of histone H3 and have also recently been reported to inactivate p53 via methylation of Lys 373.¹¹ G9a and GLP are overexpressed in various cancers,¹¹ suggesting that they are putative oncogenes and potential inhibitory targets for cancer treatment. Gaughan and colleagues¹² found that SET7/9 methylation of the androgen receptor at Lys 632 enhances transcriptional activation of target genes, that SET7/9 expression is upregulated in prostate cancer tissue, and that SET7/9 is pro-proliferative and antiapoptotic in prostate cancer cells. The non-SET HKMT, hDOT1L, methylates Lys 79 in the globular region of histone H3⁴ and is reported to be associated with leukemogenesis.¹³

The protein arginine methyltransferases (PRMTs) compose a smaller group of enzymes than the HKMTs. Only 11 isoforms have

ABBREVIATIONS: EZH2, enhancer of zeste homolog 2; FP, fluorescence polarization; GLP, G9a-like protein; ³H-SAM, S-adenosyl-L-[methyl-³H]methionine; HKMT, histone lysine methyltransferase; HMT, histone methyltransferase; HTS, high-throughput screening; IC₅₀, half-maximal inhibitory concentration; MMA, monomethyl arginine; PRMTs, protein arginine methyltransferases; SAH, S-adenosyl-L-homocysteine; SAHH, S-adenosylhomocysteine hydrolase; SAM, S-adenosyl-L-methionine; SET, Su(var)3-9, enhancer of zeste, and trithorax; uHTS, ultrahigh-throughput screening.

been discovered thus far: PRMT1–PRMT11.¹⁴ All of these enzymes display conserved sequence motifs in the catalytic domain, although methyltransferase activities have not yet been confirmed for PRMT10 and PRMT11. The PRMT enzymes have been classified according to the nature of the dimethylated arginine reaction product. The type-I PRMT enzymes catalyze the formation of monomethyl arginine (MMA) and asymmetric dimethyl arginine, while the type II PRMT enzymes form MMA and symmetric dimethyl arginine. The enzymes PRMT1, PRMT2, PRMT3, PRMT4, PRMT6, and PRMT8 belong to the type I group, whereas PRMT5, PRMT7, and PRMT9 are type II enzymes.^{15–18} Arginine methylation is an abundant post-translational modification that regulates a diverse array of cellular functions. The list of proteins known to be methylated on arginine has grown rapidly over the past decade and now includes hundreds of proteins. Recently identified PRMT substrates include nucleolin, fibrillarin, and helicases.^{17,19} Various biochemical and biological processes such as signal transduction, proliferation, transcriptional regulation, and RNA splicing are known to involve arginine methylation. In addition to the important role of PRMTs in normal cellular function, dysregulated PRMT activities are implicated in disease processes such as certain cancer types, cardiovascular disease, multiple sclerosis, and spinal muscular atrophy.^{20–22}

Due to the role of HMTs as important epigenetic regulators and their clear link to human cancers, HMTs have generated intense interest as drug discovery targets. Although many HMT assay formats are currently available, each has its own particular pros and cons (see the Discussion section), and there is no widely accepted high-throughput screening (HTS) assay format. In an effort to fill this gap, we have produced enzymes and applied a modified miniaturized radioisotope-based filter-binding assay for HMTs. HotSpotSM, originally developed for kinases,^{23,24} can be performed at the low costs necessary to serve the drug discovery market. This platform detects total methylation of any substrate on both lysine and arginine residues. Substrates ranging from peptides to nucleosomes can be used without the need for modification; therefore, this platform is suitable for ultrahigh-throughput screening (uHTS) and selectivity profiling against a large panel of HMTs. Here we will show the results of HMT studies performed with this platform. The data indicate that this format enables HTS of HMTs as well as compound evaluations and kinetic studies.

MATERIALS AND METHODS

Materials

Human DOT1L (residues 1–416; accession # NM_032482) was expressed in *Escherichia coli* as N-terminal GST fusions. Human recombinant EZH1 (residues 2–747; Genbank Accession # NM_001991) or EZH2 (residues 2–746; Genbank Accession # NM_001203247) were coexpressed with human recombinants AEBP2 (2–517; NM_001114176), EED (2–441; NM_003797), RbAp48 (2–425; NM_005610), and SUZ12 (2–739; NM_015355) in an insect cell/baculovirus expression system to form the 5-member EZH1 or EZH2 complexes. All proteins were full length (residue 2 through C-terminus). The EED subunit incorporated an N-terminal Flag-tag, and

all others included an N-terminal His-tag. Human GLP (residues 894–1298; accession # NM_024757) and Human G9a (residues 786–1210; accession # NM_006709) were expressed as N-terminal GST fusion protein in *E. coli*. Human MLL1 (residues 3745–3969; accession # NM_005933), human WDR5 (22–334; NM_017588), RbBP5 (1–538; NM_005057), Ash2L (2–534; NM_001105214), and DPY-30 (1–99; NM_0325742) were expressed in *E. coli* with N-terminal His-tags assembled as a complex and stored in 20 mM Tris-HCl, pH 7.5, 300 mM NaCl, 1 mM TCEP, 10% (w/v) glycerol, and 1 μ M ZnCl₂. Human MLL2 (residues 5319–5537; accession # NM_003482), human MLL3 (residues 4689–4911; accession # NM_170606), and human MLL4 (residues 2490–2715; accession # NM_014727) were expressed in *E. coli* with N-terminal His-tags, and SET1B (residues 1629–1923; accession # NM_015048) was expressed in *E. coli* with N-terminal GST-tag. All four were assembled in complexes as MLL1, as mentioned above. Human recombinant NSD2 (residues 2–1365; accession # NM_001042424) was expressed with an N-terminal His-tag in an insect cell/baculovirus expression system. Human recombinant SUV39H1 (residues 44–412; accession # NM_003173) and SUV39H2 (residues 48–410; accession # NM_001193424), both with C-terminal His-Tags, were expressed in *E. coli*. The following enzymes were codeveloped or purchased from BPS Biosciences: *E. coli* expressed SET7, His-tagged, full length; SET8, GST-tagged aa195–352; PRMT1, GST-tagged aa2-end; PRMT3, GST-tagged aa2-end; PRMT6, and His-tagged aa2-end, and Free StyleTM 293-F cells (human kidney line; Invitrogen) expressed SETMAR, Flag-tagged aa14-end; PRMT4, Flag-tagged aa2-end; and PRMT5, Flag-tagged aa2-end.

Nucleosomes were prepared from HeLa according to Schnitzler.²⁵ Histone H3 protein was purchased from Sigma. Chicken core histones and human recombinant histone H4 were purchased from Millipore. Histone H3 peptide aa1–21 (ART KQT ARK STG GKA PRK QLA TKA A-NH₂), histone H3 peptide aa15–39 (H-APR KQL ATK AAR KSA PAT GGV KKP H-OH), histone H4 peptide aa1–21 (H-SGR GKG GKG LGK GGA KRH RKV-OH), and histone H3 peptide aa3–17 (K9-monomethylated) were purchased from AnaSpec. [Histone peptides are henceforth referred to in the following format: H3 (1–21), H3 (15–39), etc.]

S-Adenosyl-L-[methyl-³H]methionine (³H-SAM) and streptavidin-coated FlashPlate were purchased from PerkinElmer. The control compounds S-adenosyl-L-homocysteine (SAH), Sinefungin, chaetocin, BIX01294, and suramin were purchased from Sigma. Suramin analogs, NF 110 and NF 449, were purchased from R&D Systems.

Methyltransferase Assay

Methyltransferase assays were performed in the radioisotope-based HotSpot format as described previously^{23,24} with the following modifications. The reaction buffer for EZH1 and EZH2 was 50 mM Tris-HCl, pH 8.0, 50 mM NaCl, 1 mM EDTA, 1 mM DTT, 1 mM PMSF, and 1% DMSO. The reaction buffer for all other HMTs was 50 mM Tris-HCl, pH 8.5, 50 mM NaCl, 5 mM MgCl₂, 1 mM DTT, 1 mM PMSF, and 1% DMSO. Standard substrate concentrations were 5 μ M peptide or protein substrate, and 1 μ M SAM, unless otherwise mentioned. For control compound IC₅₀ determinations, the test compounds were

diluted in DMSO, and then added to the enzyme/substrate mixtures in nanoliter amounts by using an acoustic technology (Echo550; Lab-cyte). The reaction was initiated by the addition of ^3H -SAM, and incubated at 30°C for 1 h. The reaction was detected by a filter-binding method. Data analysis was performed using GraphPad Prism software for curve fits, and GraFit (Erithacus) for global fit of kinetic studies using the ternary complex equation:

$$\nu = \frac{V_{\max}[A][B]}{K_A' \cdot K_B + K_B[A] + K_A[B] + [A][B]} \quad (1)$$

where A is SAM; B is peptide substrate; K_A and K_B are Michaelis constants for each substrate; and K_A' is the dissociation constant for SAM.

Methyltransferase assay for G9a was also performed in a Flash Plate. The reaction was performed under the same conditions as in the HotSpot assay, but using biotinylated H3 (1–21) (AnaSpec). After the termination of the reaction by the addition of 0.1 mM SAH, the reaction was transferred into the Flash Plate (PerkinElmer) and counted by TopCount (PerkinElmer).

Compound Screening

LOPAC (Sigma), a small library of 1,280 compounds, was screened against DOT1L with core histone as the substrate in the assay described as above. The compounds were tested in a single dose at 20 μM under the condition of 250 nM of DOT1L, 0.05 mg/mL of core histone, and 500 nM SAM (close to K_m) for 1-h reaction at 30°C (see *Supplementary Fig. S1* for assay optimization; *Supplementary Data* are available online at www.liebertpub.com/adt). The assay protocol is summarized in *Supplementary Table S1*.

The follow-up hit confirmation was performed in a 10-dose IC_{50} mode with a threefold serial dilution starting at 100 μM under the same condition with the primary screening.

RESULTS

Substrate Specificity

The HotSpot format measures total methylation of a substrate by direct measurement of the filter-bound tritiated substrate, without the need for coupling enzymes or antibodies. Therefore, any substrate can be used label-free. This represents a major advantage over other detection methods that require methylation-specific antibodies or peptide modifications such as biotin-labeled peptides in SPA assays and sequence manipulation in the mobility-shift assay. In addition, this radioisotope-based format is not affected by compound fluorescence or by the inhibition of coupling enzymes, the two

causes of false positives that are commonly used in approaches that monitor SAM consumption and/or SAH production.²⁶

Each lysine-specific HMT has a particular substrate specificity; each enzyme methylates specific residues on specific histones. For example, DOT1L methylates Lys 79 of histone H3,⁴ and G9a methylates Lys 9 of histone H3 and Lys 27 *in vitro*,²⁷ although methylation on proteins other than histones has been reported.¹¹ PRMTs are able to methylate arginine residues of a variety of protein substrates, including histones. To determine the proper substrates for each HMT *in vitro*, a collection of HMTs were tested against all available histone substrates. *Table 1* summarizes the substrates that showed good activity for each enzyme. In agreement with published data,²⁸ DOT1L did not methylate isolated histone H3 protein, and the activity was only seen with nucleosomes or core histones. Some enzymes only have activity with histone protein substrates or histone complexes,

Table 1. Substrate Specificity of Histone Methyltransferases

Enzyme	Substrates showing good activity in HotSpot	Reported methylation sites (from UniProtKB)
DOT1L	Nucleosomes	H3K79
EZH1	Nucleosomes, core histone, histone H3, H3 (21–44)	H3K27
EZH2	Nucleosomes, core histone, histone H3, H3 (21–44)	H3K27
G9a	Core histone, histone H3, H3 (1–21)	H3K9, H3K27, p53 K373
GLP	Core histone, histone H3, H3 (1–21)	H3K9, H3K27, p53 K373
MLL1	Nucleosomes, core histone, histone H3, H3 (1–21)	H3K4
MLL2	Nucleosomes, core histone, histone H3, H3 (1–21)	H3K4
MLL3	Nucleosomes, core histone, histone H3, H3 (1–21)	H3K4
MLL4	Nucleosomes, core histone, histone H3, H3 (1–21)	H3K4
NSD2	Nucleosomes	H3K36, H4K20
SET1B	Core histone	H3K4
SET7	Core histone, histone H3, H3 (1–21)	H3K4
SET8	Core histone, histone H4, H4 (1–21)	H4K20
SETMAR	Core histone, histone H3	H3K4, H3K36
SMYD2	Core histone, histone H3, histone H4, H3 (1–21), H4 (1–21)	H3K36
SUV39H1	Core histone, histone H3, H3 (1–21)	H3K9
SUV39H2	Core histone, histone H3, H3 (1–21)	H3K9
PRMT1	Nucleosomes, core histone, histone H4, H4 (1–21)	H4R3
PRMT3	Nucleosomes, core histone, histone H3, histone H4, H4 (1–21)	Ribosomal protein
PRMT4	Core histone, histone H3, histone H4, H3 (1–21)	H3R17
PRMT5	Core histone, histone H3, histone H4, H4 (1–21)	H2A, H3R8, H4R3
PRMT6	Histone H3, histone H4, H4 (1–21)	H3R2, H2A, H4R3

whereas others have activity with both the protein and peptide substrates. By using specifically methylated substrates, for example, dimethylated histone H3 (H3K9me2), the rates of particular methylation events (*e.g.*, H3K9me2 to H3K9me3) can also be measured.

Kinetic Studies for HMTs

Studies to determine kinetic constants, such as the K_m values of HMTs, have been reported for several assay formats. However, the values of kinetic constants may vary with the assay formats and conditions, and the reported kinetic constants of each enzyme from different assay formats can be hard to compare. The HotSpot format is essentially similar to the traditional gold standard radioisotope detection used in conjunction with gel electrophoresis or mass spectroscopy for most reported mechanistic studies. Using radioisotope-based HotSpot, the K_m was determined for several HMTs with different substrates. Reactions were performed as timecourse measurements at varying concentrations of SAM and peptide/protein substrate.

The data demonstrate that methyltransferase activities were linear with time. *Figure 1* shows the progress curves for the SUV39H2 methyltransferase reaction, as an example, plotted against time at 5 μM of peptide substrate and varied concentrations of SAM. The reaction was linear up to 60 min at most SAM concentrations, or 90 min at 1 μM SAM. Similar experiments were performed at different concentrations of the peptide substrate with varying SAM concentrations. Taking the slope of the initial linear portion (signal/time = velocity), velocities were plotted against SAM concentrations (*Fig. 2A*) or peptide substrate concentrations (*Fig. 2B*) to produce the Michaelis–Menten plots. The K_m values for SAM were not changed significantly by changing the peptide substrate concentrations (*Fig. 2A*). Similarly, the K_m values for the peptide substrate did not change over any SAM concentrations tested (*Fig. 2B*). To analyze further, the

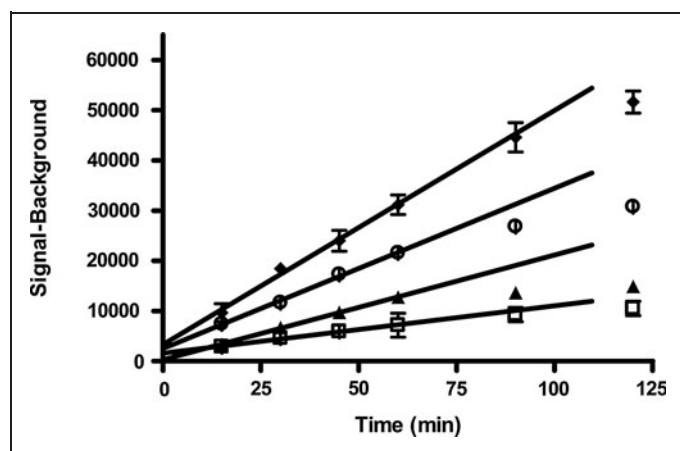


Fig. 1. Progress curves for the SUV39H2 methyltransferase reaction. Reaction conditions are 5 μM of histone H3 (aa1–21) peptide substrate and varying concentrations of *S*-adenosyl-*L*-methionine (SAM) at 0.125 μM (□), 0.25 μM (▲), 0.5 μM (○), and 1 μM (◆).

double reciprocal of *Fig. 2A* was plotted in *Fig. 2C*. As shown, lines converged at one point to the left of the *y*-axis. This pattern excludes a possibility of double-displacement reactions (or Ping-Pong; first, the substrate/product must leave before second substrate binding), which would display parallel lines in double-reciprocal plots.²⁹ Therefore, the SUV39H2 methyltransferase reaction must be a random-ordered or compulsory-ordered Bi-Bi reaction, which means that SUV39H2 forms a ternary complex of the SUV39H2/SAM/peptide substrate. At this point, it is difficult to distinguish between the two mechanisms: random ordered or compulsory ordered. To obtain accurate constants, a global-fit analysis was performed using GraFit software with the ternary complex equation (*Eq. 1*; *Fig. 2D*). Global fits weigh equally on all data points; therefore, it is more reliable than the traditional graphical method, which is highly affected by imprecise low-activity data points. The global fits revealed that the K_m value of SUV39H2 for SAM was 1.27 μM , and that for the peptide was 9.9 μM (*Fig. 2D*). Further studies with protein or methylated substrates are needed to understand the mechanism of the SUV39H2 reaction in more detail, to determine, for example, whether the reaction is processive or not (*i.e.*, different substrates with protein and/or methylated substrate, processive or not).

The kinetic constants for other HMTs were determined by similar experiments. Most methyltransferase reactions were linear with time up to 60 min, and others for even longer, up to 90–120 min. Taking slopes of the initial linear portion of the reaction progress curves, the Michaelis–Menten plots were obtained for other HMTs with their corresponding substrates. The obtained K_m values by global fit are summarized in *Table 2*. The K_m value of SET7 for SAM was lower^{30,31} or higher³² than that reported previously, depending on the assay format. The SAM K_m values for all HMTs tested were lower than 5 μM , mostly lower than 1 μM under the conditions tested. Similarly, with a couple of exceptions, the K_m values for peptide or protein substrates were lower than 1 μM (*Table 2*). The kinetic constants of alternative substrates with the listed HMTs as well as the kinetic characterization of additional HMTs were determined. In general, the K_m values for the protein substrate were low and difficult to obtain accurately. Thus, the SAM K_m values were obtained at a fixed substrate concentration (*Table 3*). The SAM K_m values at fixed substrate concentrations fall in a similar range to those in *Table 2*, and are in generally a good agreement with reported values obtained by radioisotope-based assays.³²

Compound Evaluation

The known methyltransferase inhibitors were tested in this assay format against selected HMTs: G9a, SET7, and PRMT5. The compounds tested were SAH (*S*-Adenosyl-*L*-homocysteine or AdoHcy), sinefungin, chaetocin, and BIX01294. SAH is a product of the methyltransferase reaction, which inhibits HMTs competitively with respect to SAM. Sinefungin, a fungal compound, is an analog of cofactor SAM, chaetocin, an inhibitor of SUV39, and BIX01294, an inhibitor of G9a/GLP.^{33–35} As shown in *Fig. 3*, the IC_{50} values for G9a, SET7, and PRMT5 with peptide and protein substrates are obtained

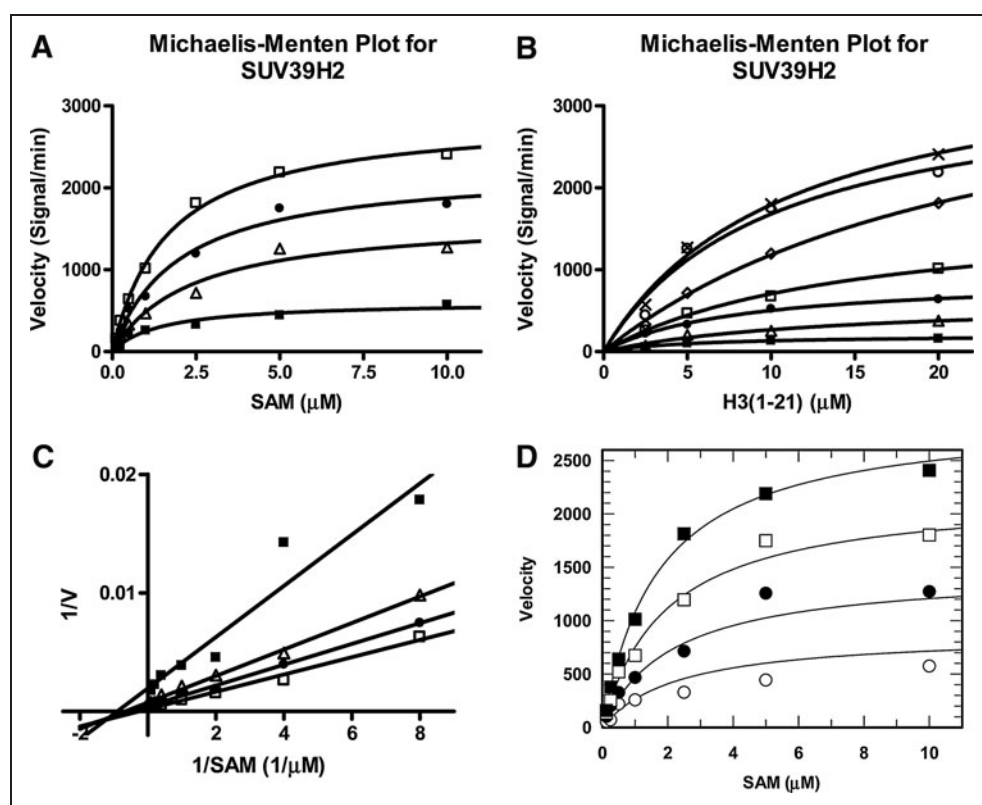


Fig. 2. Kinetic analysis of SUV39H2 with a peptide substrate. The initial velocity of the SUV39H2 reaction was plotted as the Michaelis–Menten plots for SAM (**A**) and for histone H3 (aa1–21) peptide substrate (**B**) using GraphPad Prism software. Peptide concentrations and K_m values obtained by individual nonlinear regression in (**A**) are 2.5 and 1.46 (\blacksquare), 5 and 2.38 (\triangle), 10 and 2.00 (\bullet), and 20 and 1.67 μM (\square), respectively. SAM concentrations and obtained K_m values in (**B**) are 0.125 and 5.77 (\blacksquare), 0.25 and 13.6 (\triangle), 0.5 and 8.14 (\bullet), 1 and 14.53 (\square), 2.5 and 23.6 (\diamond), 5 and 10.1 (\circ), and 10 and 10.9 μM (\times), respectively. Data from (**A**) were replotted as a double-reciprocal plot (**C**: symbols are corresponding to **A**), and global-fit (**D**) using GraFit software with the ternary complex equation (Eq. 1). Peptide concentrations in (**D**) are 2.5 (\circ), 5 (\bullet), 10 (\square), and 20 μM (\blacksquare), and K_m for SAM is 1.27 μM , and K_m for peptide substrate is 9.90 μM , and the dissociation constant for SAM, K_A' , is 2.58 μM .

using the HotSpot radioisotope-based assay under the standard conditions. SAH and sinefungin each differed in their inhibition, although both compounds were SAM competitive: IC_{50} values of 1.4 μM and 10 μM for G9a, 290 μM and 2.4 μM for SET7, and 1.2 μM and 306 nM for PRMT5, respectively, with a peptide substrate.

Table 2. Kinetic Constants for Histone Methyltransferases: Constants Obtained from Global Fit

Enzyme	Substrate	SAM K_m (μM)	Substrate K_m (μM)
DOT1L	Core Histone	0.38 \pm 0.053	0.061 \pm 0.012 (mg/mL)
EZH2	Core Histone	0.42 \pm 0.072	0.012 \pm 0.005 (mg/mL)
G9a	H3(1–21) peptide	0.53 \pm 0.043	0.6 \pm 0.096
SET7	H3(1–21) peptide	0.22 \pm 0.074	5.7 \pm 0.031
SUV39H1	Histone H3	0.56 \pm 0.014	0.53 \pm 0.042
SUV39H2	H3(1–21) peptide	1.27 \pm 0.56	9.9 \pm 0.92
PRMT1	H4(1–21) peptide	0.28 \pm 0.047	0.24 \pm 0.089
PRMT3	H4(1–21) peptide	2.1 \pm 0.67	0.54 \pm 0.086
PRMT4	H3(1–21) peptide	3.1 \pm 0.46	0.32 \pm 0.069
PRMT5	H4(1–21) peptide	1.07 \pm 0.21	0.11 \pm 0.075

SAM, S-adenosyl-L-methionine.

Chaetocin inhibited both G9a and SET7 weakly with a peptide substrate (IC_{50} values of 18 μM and 540 μM , respectively), but did not inhibit PRMT5. Interestingly, the G9a inhibitor BIX01294 also weakly inhibited SET7 and PRMT5 with a peptide substrate, but did not inhibit with a protein substrate. The IC_{50} value of BIX01294 for G9a with a peptide substrate was 5.3 μM (Fig. 3A), slightly higher than that reported.³⁵ To validate the G9a assay with a peptide substrate in HotSpot, the G9a assay was also performed in the FlashPlate format with 0.5 μM of biotinylated H3 (1–21) peptide at 1 μM SAM. The IC_{50} value of BIX01294 was obtained with 5.0 μM , comparable with the value obtained with HotSpot (Fig. 3A).

When the histone H3 protein was used as a substrate, the IC_{50} values were shifted up for most compounds, especially for BIX01294 (Fig. 3B, D, F). These results suggest that the K_m value for the histone protein was lower than that of the peptide substrate, thus making it more difficult for BIX01294 to displace the histone protein.

Since BIX01294 has been reported as a peptide substrate-competitive and SAM-uncompetitive inhibitor,³³ lower peptide (0.5 μM) and higher SAM (10 μM) concentrations were tested (Fig. 4A). Under this condition, the IC_{50} value was shifted to a lower value, 2.2 μM , which is similar to that obtained by a mass spectrometry-based assay.³⁴ On the other hand, the IC_{50} value of SAH was shifted 10-fold higher when the SAM concentration was increased to 10 μM (Fig. 4A). This shift was expected for a SAM competitive inhibitor. G9a can mono- and dimethylate the lysine 9 residue on histone H3. Therefore, dimethylation was monitored using monomethylated lysine 9 peptide as a substrate. As shown in Fig. 4B, the IC_{50} value of BIX01294 was

Table 3. Kinetic Constants for Histone Methyltransferases: S-Adenosyl-L-Methionine K_m at a Fixed Substrate Concentration

Enzyme	Substrate	SAM K_m (μM)
EZH1	Histone H3	1.24 ± 0.15
EZH2	Histone H3	1.64 ± 0.26
G9a	Histone H3	0.74 ± 0.10
GLP	Core histone	0.95 ± 0.18
GLP	Histone H3	0.29 ± 0.066
MLL1	Core histone	0.66 ± 0.14
MLL1	Histone H3	0.50 ± 0.067
MLL2	Core histone	4.50 ± 0.82
MLL2	Histone H3	3.17 ± 0.37
MLL3	Core histone	0.85 ± 0.19
MLL3	Histone H3	0.96 ± 0.18
SET7	Histone H3	1.64 ± 0.12
SET8	Histone H4	16.3 ± 5.83
SETMAR	Histone H3	1.13 ± 0.42
SMYD2	Histone H3	0.12 ± 0.013
SUV39H1	Histone H3	0.75 ± 0.11
SUV39H2	Histone H3	0.74 ± 0.23
PRMT1	Histone H4	5.20 ± 0.91
PRMT3	Histone H3	2.80 ± 0.61
PRMT4	Histone H3	0.21 ± 0.052
PRMT5	Histone H3	0.70 ± 0.17
PRMT6	Histone H3	2.20 ± 0.47

Kinetic constants were determined at a concentration of 5 μM for histone or 0.05 mg/mL for core histone.

shifted about fivefold lower to 1.3 μM compared to that with non-methylated substrate (Fig. 3A), although the activity was <1/10. Trimethylation was minimal when using dimethylated lysine 9 peptide as a substrate under this condition. On the other hand, the IC_{50} value of SAH was not changed significantly (Figs. 3A and 4B).

Overall, the data indicate that the HotSpot format is ideal for compound profiling, since any substrate can be used without any modifications. In addition, the IC_{50} values obtained with this format are similar to those from mass spectrometry-based assays, which are the most reliable methods for detecting the methyltransferase reactions.

Compound Screening

Low-cost and robust assays with minimal false positives have been desired for HTS, especially for difficult or expensive enzymes. DOT1L is an attractive drug target; however, it needs a histone octamer or nucleosomes as a substrate for enzyme activity, and monomer histone or peptide substrates do not work. Thus, screening against DOT1L is costly and difficult to run with certain assay formats. We screened LOPAC (Sigma), a small library of 1,280 compounds, against DOT1L with core histone as the substrate in a miniaturized gold-standard radioisotope-based assay where the cost of the radioisotope-labeled cofactor and its waste, as well as that of the other reagents, could be minimized. Although most HMT assays in this format have Z' -factors³⁶ of >0.6, the Z' -factor was 0.52 for the DOT1L assay, and the Signal:Background ratio was 4.3 (Supplementary Table S2). We identified three compounds that showed more than 70% inhibition against DOT1L—two of these were suramin and its analog, while the other was L-cysteine sulfinic acid.

The follow-up hit confirmation was performed by cherry-picking of three compounds under the same condition of primary screening. Then, suramin and its 2 analogs, NF 110 and NF 449, were profiled against 17 HMTs in our panel. The obtained IC_{50} values are summarized in Table 4. Suramin and NF 449 showed similar inhibition patterns, whereas NF 110 showed little activity. Interestingly, activities of many HMTs were increased by suramin and NF 449 at low concentrations of compounds, while inhibited at higher concentrations. The degree of such activations was not consistent; thus, the IC_{50} values may not be accurate; these were expressed in italic letters. The reason for such activations is not clear, whether there was real enzyme activation, or were false signals caused by compound aggregation, etc. Since suramin is a relatively large molecule, it could possibly have caused compound aggregation involving substrates and/or enzymes. Methyltransferases that were consistently inhibited by suramin (without apparent activation) are DOT1L, NSD2, and PRMT4 with IC_{50} values at a low μM range.

DISCUSSION

The radioisotope-based miniaturized filter-binding assay, HotSpot platform, was initially developed for kinase assays, but has since been successfully applied to other transferase enzyme classes to serve markets for uHTS, large-scale IC_{50} determinations, and selectivity/toxicity profiling in drug discovery.^{23,24} In this study, we have modified this platform for HMT assays using tritium-labeled SAM as a cofactor, and demonstrated that compound profiling, kinetic studies, and HTS can be performed cost effectively with this system.

The currently available assay formats for HMTs have various limitations.²⁶ The traditional methods are gel-based radioisotope assays or mass spectrometry-based assays,³⁷ which directly measure methylation on the substrate. Mass spectrometry-based assays are the most reliable assays, and therefore detailed kinetic studies still employ these formats. However, applying high-throughput formats with these assays is difficult and/or requires expensive instrumentation. Another radioisotope-based assay, first reported by Rathert *et al.*,³⁸

used streptavidin-coated FlashPlates to capture the biotinylated peptide substrate, which, while bound to the plate, was enzymatically labeled with tritiated SAM. This is a continuous assay and may be applied to HTS. Aside from the requirement for biotinylated peptides, it is hard to control the substrate concentrations in this system, making the determination of kinetic parameters problematic.

Most popular assays are antibody based and employ a variety of detection systems, including biotin-avidin, CLOT, and ELISA. The CLOT assay is a homogeneous assay in which the methylation of a biotinylated histone peptide is measured through methylation-specific antibody-based detection, in conjunction with streptavidin-coated donor and secondary antibody-coated AlphaScreen acceptor beads.³⁹ The limitation of such antibody-based detection systems is the need for antibodies specific for particular methylation sites as well as for mono-, di-, or trimethylation.

Therefore, it is difficult to profile a compound against a wide selection of HMTs with different substrates/methylation sites or to perform kinetic studies. While the above methods detect methylation of (mostly) peptide substrates, another approach is to detect AdoHcy (*S*-adenosyl-homocysteine, or SAH), the reaction product derived from AdoMet (SAM). Graves *et al.*⁴⁰ have described a competitive fluorescence polarization (FP) assay that uses an antibody against AdoHcy and a fluorophore-conjugated AdoHcy. The fluorescent AdoHcy conjugate is bound by the anti-AdoHcy-antibody to produce a high FP complex: The AdoHcy produced in the methylation process displaces the fluorescent tracer, resulting in a decrease of the FP signal. Although the assay is homogenous and continuous, its sensitivity is low. Collazo *et al.*⁴¹ have reported an enzyme-coupled assay that utilizes *S*-adenosylhomocysteine hydrolase (SAHH) to hydrolyze the methyltransferase product, AdoHcy, to homocysteine (Hcy) and adenosine (Ado), and adenosine deaminase to pull the reaction to completion. The Hcy concentration is then determined through conjugation of its free sulfhydryl moiety to a thiol-sensitive fluorophore (ThioGlo). One disadvantage of this assay is its sensitivity to thiol-based reducing agents (*e.g.*, DTT or β -mercaptoethanol), including thiol-containing compounds. A disadvantage of enzyme-coupled assays

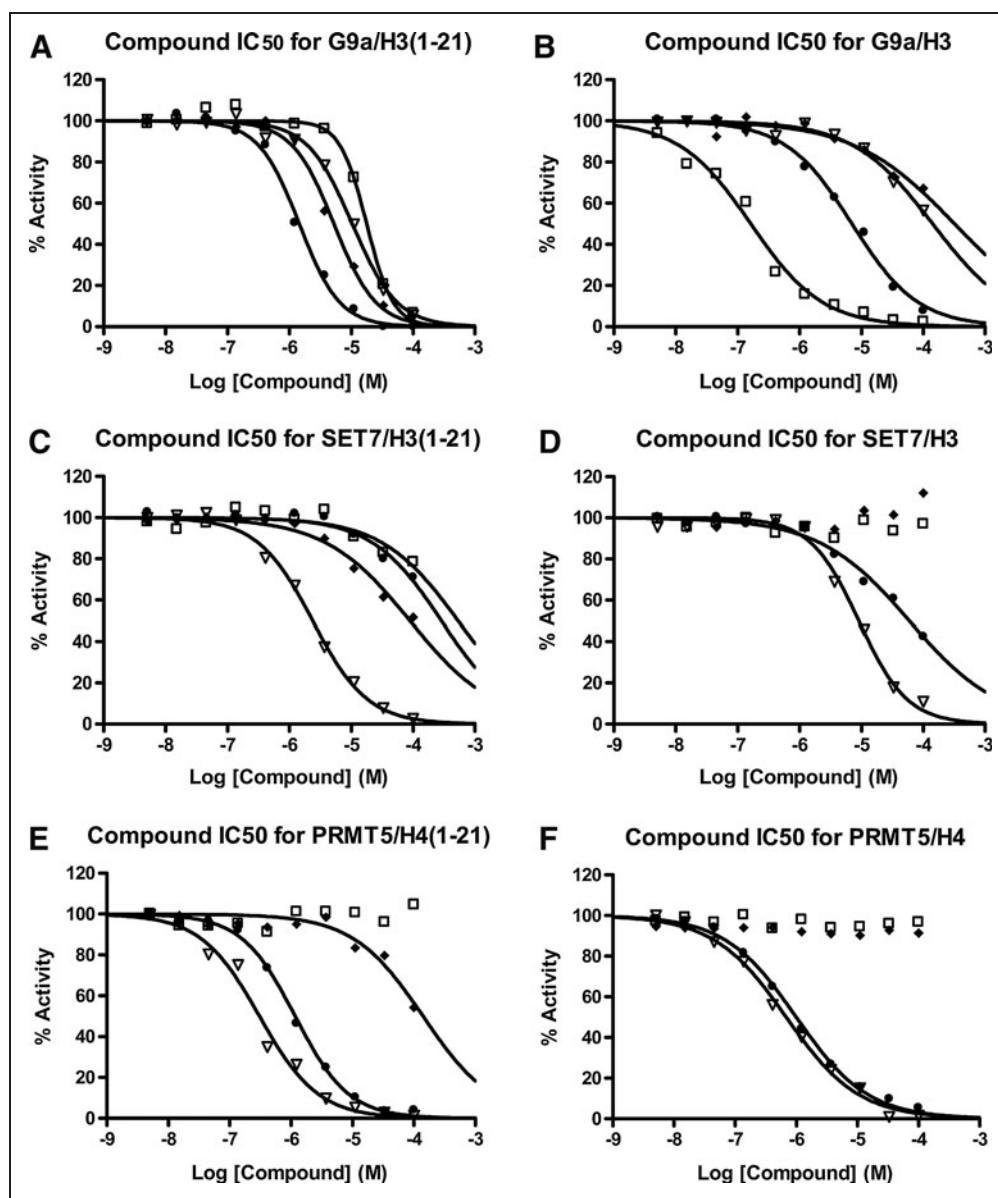
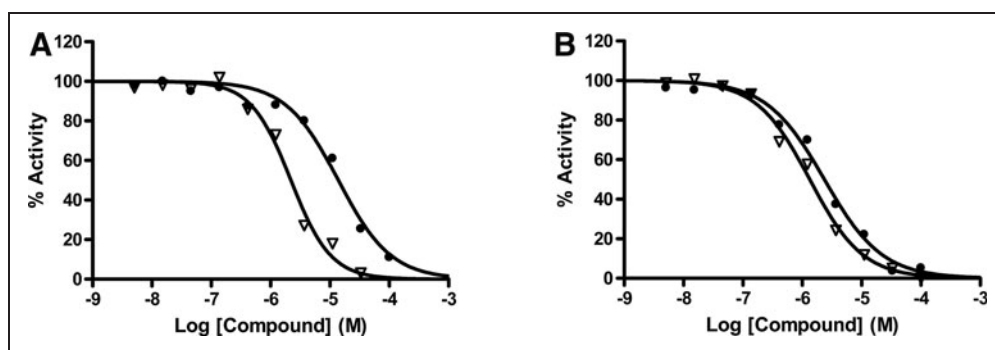


Fig. 3. The IC_{50} determinations of control compounds for G9a, SET7, and PRMT5 at $1 \mu M$ SAM with peptide or protein substrates; (A) G9a and (C) SET7 with $5 \mu M$ of histone H3 (aa1–21) peptide as substrate, (E) PRMT5 with $5 \mu M$ of histone H4 (aa1–21) peptide as substrate, (B) G9a and SET7 (D) with $5 \mu M$ histone H3 as substrate, (F) and PRMT5 with $5 \mu M$ of histone H4. Compounds tested are SAH (●), sinefungin (▽), BIX01294 (◆), and chaetocin (□), and the obtained IC_{50} values are (A) 1.45, 10.4, 5.3, and $17.8 \mu M$, respectively, (B) 7.1, 150, 320, and $0.16 \mu M$, respectively, (C) 290, 2.38, 89.1, and $540 \mu M$, respectively, (D) $60 \mu M$ for SAH and $9.1 \mu M$ for sinefungin, (E) $1.2 \mu M$ for SAH, $0.31 \mu M$ for sinefungin, and $140 \mu M$ for BIX01294, and (F) $1.0 \mu M$ for SAH and $0.69 \mu M$ for sinefungin.

FIG. 4. The IC_{50} determinations of control compounds for G9a under different conditions. **(A)** G9a with 0.5 μ M of histone H3 (aa1–21) peptide as a substrate at 10 μ M SAM, and **(B)** G9a with 5 μ M of histone H3 (aa1–21; K9-monomethylated) peptide as substrate. The obtained IC_{50} values are **(A)** 13.9 μ M for SAH (●) and 2.2 μ M for BIX01294 (▽), **(B)** 2.4 and 1.3 μ M, respectively.



in general is the possibility of false positives, which are inhibitors of the coupling enzymes rather than the screening target, and the consequent need for counter assays for the coupling enzymes. In addition, the coupling enzyme should not be rate limiting to the overall reaction: SAHH, however, is a very slow enzyme. A further

disadvantage of the SAHH/ThioGlo system, which applies equally to any system based on fluorescence detection, is that fluorescence or fluorescence quenching from screening compounds may interfere with the assay. The mobility-shift assay⁴² and the FLEXYTE™ Fluorescence Lifetime assay have also been reported for G9a

screening, requiring a protease to digest the unmethylated substrate for detection. These assays not only require specially designed artificial substrates, but also require counter screening for the coupling proteases. Further, a lack of hit overlap with the FlashPlate assay has been reported.⁴³ All of the disadvantages described above are minimized in the gold-standard miniaturized radioisotope-based HotSpot format. Since this format is based on the filter-binding capture of substrates, the only limitation is the capacity of the filter binding. However, the linear binding range is much larger than that of the FlashPlate. This can be overcome by diluting the reaction mixture before applying on the filter when the substrate concentration exceeds the binding capacity. The binding capacity and a linear range can be measured easily by a standard curve of known concentrations of substrates.

The IC_{50} value of G9a inhibitor, BIX01294, was originally reported as 2.7 μ M for G9a with the DELFIA assay.³³ Later, IC_{50} values of 1.9 μ M, 180 nM, and 250 nM were reported with mass spectrometry [10 μ M Histone H3 (1–15) at 100 μ M SAM],³⁴ enzyme-coupled assays [5 μ M H3 (1–25) at 16 μ M SAM], and CLOT assays [0.5 μ M biotin-H3 (1–11) at 20 μ M SAM],³⁵ respectively. Utilizing the HotSpot format [a standard condition of 5 μ M H3 (1–21) at 1 μ M SAM], we obtained an IC_{50} value of 5.3 μ M (Fig. 3A). Considering the competitive mode of BIX01294 inhibition with respect to the peptide substrate and the K_m for peptide (0.6 μ M in the Table 2), the K_i value of

Table 4. Methyltransferase Profiling for Suramin and Analogs

Target	Substrate	Suramin	NF110	NF449	SAH
DOT1L	Core histone	2.12±0.50	—	6.54±0.91	1.79±0.74
EZH1	Core histone	45.9±20	100±31	36.2±15	18.0±0.50
EZH2	Core histone	11.5±10	116±15	13.6±10	11.6±2.1
G9a	Histone H3	29.5±5.2	198±22	39.4±7.4	3.66±0.07
GLP	Core histone	3.64±0.86	—	2.95±0.52	0.24±0.01
NSD2	Nucleosomes	0.32±0.04	—	1.66±0.42	2.06±0.30
SET1B	Core histone	3.48±1.02	—	1.92±1.3	3.20±0.68
SET7	Histone H3	4.94±1.14	—	11.6±2.4	61.1±9.6
SET8	Histone H4	—	14.8±4.5	—	55.1±16
SUV39H1	Histone H3	54.6±14	—	144±42	50.5±11
SUV39H2	Histone H3	30.3±12	—	—	45.6±12
PRMT1	Histone H4	7.50±2.1	—	8.76±2.4	0.39±0.10
PRMT3	Histone H3	10.4±2.4	—	11.2±2.8	1.94±0.52
PRMT4	Histone H3	1.51±0.45	—	1.27±0.22	0.12±0.04
PRMT5	Histone H3	33.2±11	—	—	1.66±0.5
PRMT6	Histone H3	3.32±0.12	—	3.35±0.03	0.08±0.03
SETMAR	Histone H3	21.0±7.2	—	23.9±2.8	0.22±0.05
SMYD2	Histone H3	1.18±0.1	—	1.07±0.04	0.32±0.1

Profiles are reported as IC_{50} , in μ M. Boldface and italics indicate consistent and inconsistent inhibitions, respectively (see the text).

SAH, S-adenosyl-L-homocysteine.

BIX01294 is estimated as 570 nM, in good agreement with published data at low peptide concentrations.³⁵ Since it has been reported that BIX01294 is competitive with the peptide substrate, but uncompetitive with SAM,³³ the IC₅₀ value was determined under lower peptide and higher SAM concentrations. Under this condition [0.5 μM H3 (1–21) at 10 μM SAM], the IC₅₀ value was 2.2 μM (Fig. 4A), shifted about twofold, which is close to the value obtained by mass spectrometry.³⁴ Interestingly, the IC₅₀ value was shifted about fourfold lower when the substrate was monomethylated (Figs. 3A vs. 4B). However, the IC₅₀ values are still higher than those compared to the values obtained by an SAHH-coupling assay or CLOT assay.³⁵ In assays using the AlphaLISA technique, the IC₅₀ value of BIX01294 against G9a (2.2 μM) was also higher (PerkinElmer, AlphaLISA Technical Note #2). We have performed another radioisotope-based assay using streptavidin-coated FlashPlate with biotinylated histone H3 peptide, and obtained similar results to those from the HotSpot assay. When using histone H3 protein as substrate, the IC₅₀ value was shifted 80-fold higher (Fig. 3B). These shifts may be caused by the change in binding affinity to substrates, since BIX01294 is a competitive inhibitor with respect to the peptide substrate.³³ As it is expected that the binding affinity would increase for a protein substrate relative to a peptide, the increased IC₅₀ value for a peptide/protein competitive inhibitor would make sense, consistent with a very low *K_m* value for the protein substrate. In fact, it was very hard to obtain the *K_m* values for the protein substrate for most HMTs. Shinkai and Tachibana⁴⁴ have also observed that the inhibition of G9a by BIX01294 is robust if an H3 N-terminal oligopeptide is used as a substrate for the *in vitro* methyltransferase assay, but is not significant (no inhibition at 10 μM) if a full-length H3 is used. It would be interesting to determine the processivity of G9a methyltransferase activity with a protein substrate in the presence and absence of BIX01294. Further studies are needed to elucidate the mechanism of action of BIX01294 (and recently found analogs) not only with a peptide substrate, but with a protein substrate as well.

The data in this study demonstrate the capability of the HotSpot platform when applied to the histone methyltransferase assays. The data quality is sufficient for all drug discovery activities, from ultra-high throughput screening to compound profiling against a large collection of HMTs and kinetic studies. Advantageous features of this platform for drug discovery include the absence of interference from fluorescent compounds and the elimination of the need for coupling enzymes, specific antibodies, or specifically modified peptide substrates. This enables substrate profiling as well as the determination of total methylation with unidentified protein substrates or with known peptides/proteins at undetermined methylation sites. Taking these advantages, one can perform compound screening at *K_m* of peptide or SAM, or profiling under conditions close to *in vivo* using nucleosomes as the substrate. One concern may be data reproducibility when using nucleosomes or core histone as a substrate, since they are purified from natural sources (HeLa or chicken, respectively). Although their methylation states are unknown, data reproducibility was satisfactory (the data consistency of the IC₅₀ values for SAH was

shown in *Supplementary Table S3*); presumably, preparations are well homogenized and minimal lot-to-lot variability. Since the platform is a miniaturized radioisotope-based assay, it reduces the cost by minimizing reagent usage. This is a considerable advantage especially for difficult or expensive enzymes and substrates. We performed a small-library HTS against DOT1L, which requires a special substrate, core histones, and suramin was identified as a DOT1L inhibitor. Subsequently, suramin was profiled against 17 methyltransferases with different substrates. Since the major advantage of this assay format is that it can be applied universally to methyltransferases regardless of the substrate, it is suitable for profiling. Although the activities of some HMTs are increased at low concentrations, methyltransferases that were consistently inhibited (without apparent activation) by suramin are DOT1L, NSD2, and PRMT4 with IC₅₀ values at a low μM range (Table 4). This is the first finding that suramin inhibits DOT1L and NSD2 activities, although it has been reported very recently that a few HMTs are inhibited by a suramin analog using a peptide as the substrate.⁴⁵ Suramin is an old drug that has been used for the treatment of trypanosomiasis and is known as an antagonist of P2 receptors; recently, the application of suramin to cancer treatment has been explored.⁴⁶ It would be interesting to determine the effects of suramin on methylation states at the cellular level, especially in cancer cell lines.

ACKNOWLEDGMENT

This work was funded in part by NIH SBIR grants R44CA139621 to H.M.

DISCLOSURE STATEMENT

No competing financial interests exist.

REFERENCES

- Luger K, Mäder A, Richmond RK, Sargent DF, Richmond TJ: Structure of the nucleosome core particle at 2.8Å resolution. *Nature* 1997;389:251–260.
- Rea S, Eisenhaber F, O'Carroll D, et al.: Regulation of chromatin structure by site-specific histone H3 methyltransferases. *Nature* 2000;406:593–599.
- Lund AH, van Lohuizen M: Polycomb complexes and silencing mechanisms. *Curr Opin Cell Biol* 2004;16:239–246.
- Feng Q, Wang H, Ng HH, et al.: Methylation of H3-lysine 79 is mediated by a new family of HMTases without a SET domain. *Curr Biol* 2002;12:1052–1058.
- Lund AH, van Lohuizen M: Epigenetics and cancer. *Genes Dev* 2004;18:2315–2335.
- Copeland RA, Solomon ME, Richon VM: Protein methyltransferases as a target class for drug discovery. *Nat Rev Drug Discov* 2009;8:724–732.
- Margueron R, Li G, Sarma K, et al.: Ezh1 and Ezh2 maintain repressive chromatin through different mechanisms. *Mol Cell* 2008;32:503–518.
- Cao R, Wang L, Wang H, et al.: Role of histone H3 lysine 27 methylation in Polycomb-group silencing. *Science* 2002;298:1039–1043.
- Kuzmichev A, Jenuwein T, Tempst P, Reinberg D: Different EZH2-containing complexes target methylation of histone H1 or nucleosomal histone H3. *Mol Cell* 2004;14:183–193.
- Ernst T, Chase AJ, Score J, et al.: Inactivating mutations of the histone methyltransferase gene EZH2 in myeloid disorders. *Nat Genet* 2010;42:722–726.
- Huang J, Dorsey J, Chuikov S, et al.: G9a and Glp Methylate Lysine 373 in the Tumor Suppressor p53. *J Biol Chem* 2010;285:9636–9641.

12. Gaughan L, Stockley J, Wang N, et al.: Regulation of the androgen receptor by SET9-mediated methylation. *Nucleic Acids Res* 2011;39:1266–1279.
13. Okada Y, Feng Q, Lin Y, et al.: hDOT1L links histone methylation to leukemogenesis. *Cell* 2005;121:167–178.
14. Wolf SS: The protein arginine methyltransferase family: an update about function, new perspectives and the physiological role in humans. *Cell Mol Life Sci* 2009;66:2109–2121.
15. Krause CD, Yang Z-H, Kim Y-S, Lee J-H, Cook JR, Pestka S: Protein arginine methyltransferases: evolution and assessment of their pharmacological and therapeutic potential. *Pharmacol Ther* 2007;113:50–87.
16. Trojer P, Dangl M, Bauer I, Graessle S, Loidl P, Brosch G: Histone methyltransferases in *Aspergillus nidulans*: evidence for a novel enzyme with a unique substrate specificity. *Biochemistry* 2004;43:10834–10843.
17. Pahlich S, Zakaryan RP, Gehling H: Protein arginine methylation: cellular functions and methods of analysis. *Biochim Biophys Acta* 2006;1764:1890–1903.
18. Lakowski, TM, Frankel, A: Kinetic analysis of human protein arginine methyltransferase 2: formation of monomethyl and asymmetric dimethyl-arginine residues on histone 4. *Biochem J* 2009;421:253–261.
19. Paik WK, Paik DC, Kim S: Historical review: the field of protein methylation. *Trends Biochem Sci* 2007;32:146–152.
20. Gary JD, Clarke S: RNA and protein interactions modulated by protein arginine methylation. *Prog Nucleic Acid Res Mol Biol* 1998;61:65–131.
21. Aletta JM, Hu JC: Protein arginine methylation in health and disease. *Biotechnol Annu Rev* 2008;14:203–224.
22. Bhaumik SR, Smith E, Shilatifard A: Covalent modifications of histones during development and disease pathogenesis. *Nat Struct Mol Biol* 2007;14:1008–1016.
23. Ma H, Deacon SW, Horiuchi KY: The challenge of selecting protein kinase assays for lead discovery optimization. *Expert Opin Drug Discov* 2008;3:607–621.
24. Anastassiadis T, Deacon SW, Devarajan K, Ma H, Peterson JR: Comprehensive assay of kinase catalytic activity reveals features of kinase inhibitor selectivity. *Nat Biotech* 2011;29:1039–1045.
25. Schnitzler GR: *Isolation of Histones and Nucleosome Cores from Mammalian Cells*. *Current Protocols in Molecular Biology*. New York: John Wiley & Sons, Inc., 2000;21.5.1–21.5.12.
26. Luo M: Current chemical biology approaches to interrogate protein methyltransferases. *ACS Chem Biol* 2012;7:443–463.
27. Tachibana M, Sugimoto K, Fukushima T, Shinkai Y: Set domain-containing protein, G9a, is a novel lysine-preferring mammalian histone methyltransferase with hyperactivity and specific selectivity to lysines 9 and 27 of histone H3. *J Biol Chem* 2001;276:25309–25317.
28. Fingerman IM, Li H-C, Briggs SD: A charge-based interaction between histone H4 and Dot1 is required for H3K79 methylation and telomere silencing: identification of a new *trans*-histone pathway. *Genes Dev* 2007;21:2018–2029.
29. Segel IH: Chapter 9: Steady-state kinetics of multireactant enzymes. In Segel IH (ed): *Enzyme Kinetics*. New York: John Wiley & Sons Inc., 1975;506–841.
30. Trievel RC, Beach BM, Dirk LMA, Houtz RL, Hurley JH: Structure and catalytic mechanism of a SET domain protein methyltransferase. *Cell* 2002;111:91–103.
31. Dirk LMA, Flynn EM, Dietzel K, Couture J-F, Trievel RC, Houtz RL: Kinetic manifestation of processivity during multiple methylations catalyzed by SET domain protein methyltransferases. *Biochemistry* 2007;46:3905–3915.
32. Richon VM, Johnston D, Sneeringer CJ, et al.: Chemogenetic analysis of human protein methyltransferases. *Chem Biol Drug Des* 2011;78:199–210.
33. Kubicek S, O'Sullivan RJ, August EM, et al.: Reversal of H3K9me2 by a small-molecule inhibitor for the G9a histone methyltransferase. *Mol Cell* 2007;25:473–481.
34. Chang Y, Zhang X, Horton JR, et al.: Structural basis for G9a-like protein lysine methyltransferase inhibition by BIX-01294. *Nat Struct Mol Biol* 2009;16:312–317.
35. Liu F, Chen X, Allali-Hassani A, et al.: Protein lysine methyltransferase G9a inhibitors: design, synthesis, and structure activity relationships of 2,4-diamino-7-aminoalkoxy-quinazolines. *J Med Chem* 2010;53:5844–5857.
36. Zhang JH, Chung TDY, Oldenburg KR: A simple statistical parameter for use in evaluation and validation of high-throughput screening assays. *J Biomol Screen* 1999;4:67–73.
37. Bonaldi T, Regula JT, Imhof A: The use of mass spectrometry for the analysis of histone modifications. *Methods Enzymol* 2004;377:111–130.
38. Rathert P, Cheng X, Jeltsch A: Continuous enzymatic assay for histone lysine methyltransferases. *BioTechniques* 2007;43:602–608.
39. Quinn AM, Allali-Hassani A, Vedadi M, Simeonov A: A chemiluminescence-based method for identification of histone lysine methyltransferase inhibitors. *Mol Biosyst* 2010;6:782–788.
40. Graves TL, Zhang Y, Scott JE: A universal competitive fluorescence polarization activity assay for S-adenosylmethionine utilizing methyltransferases. *Anal Biochem* 2008;373:296–306.
41. Collazo E, Couture JF, Bulfer S, Trievel RC: A coupled fluorescent assay for histone methyltransferases. *Anal Biochem* 2005;342:86–92.
42. Wigle TJ, Provencher LM, Norris JL, et al.: Accessing protein methyltransferase and demethylase enzymology using microfluidic capillary electrophoresis. *Chem Biol* 2010;17:695–704.
43. Hilyard K, Beyer KS, Ahrens T, Bergner A, Fasler S, Hafenbradl D: Epigenetic protein targets: Computational approaches and new assay technologies for efficient hit finding against G9a and LSD1. 2012 BioFocus web poster. [www.biofocus.com/_downloads/posters/2012/epigenetic-protein-targets .pdf](http://www.biofocus.com/_downloads/posters/2012/epigenetic-protein-targets.pdf)
44. Shinkai Y, Tachibana M: H3K9 methyltransferase G9a and the related molecule GLP. *Genes Dev* 2011;25:781–788.
45. Ibanez G, Shum D, Blum G, et al.: A high throughput scintillation proximity imaging assay for protein methyltransferases. *Comb Chem High Throughput Screen* 2012;15:359–371.
46. McGeary RP, Bennett AJ, Tran QB, Cosgrove KL, Ross BP: Suramin: clinical uses and structure-activity relationships. *Mini Rev Med Chem* 2008;8:1384–1394.

Address correspondence to:

Kurumi Y. Horiuchi, PhD, or Haiching Ma, PhD
 Department of Biochemistry
 Reaction Biology Corporation
 One Great Valley Parkway, Suite 2
 Malvern, PA 19355

E-mail: kurumi.horiuchi@reactionbiology.com
 or haiching.ma@reactionbiology.com